International Journal of Mechanical, Industrial and Aerospace Sciences
ISSN: 2517-9950
Vol:3, No:7, 2009

The Self-Propelled Model of a Boat, Based on the Wave Thrust

V. Arabadzhi

Abstract**—**We attempted investigate a boat model, based on the conversion of energy of surface wave into a sequence of unidirectional pulses of jet spurts, in other words - model of the boat, which is thrusting by the waves field on water surface. These pulses are forming some average reactive stream from the output nozzle on the stern of boat. The suggested model provides the conversion of its oscillatory motions (both pitching and rolling) into a jet flow. This becomes possible due to special construction of the boat and due to several details, sensitive to the local wave field. The boat model presents the uniflow jet engine without slow conversions of mechanical energy into intermediate forms and without any external sources of energy (besides surface waves). Motion of boat is characterized by fast jerks and average onward velocity, which exceeds the velocities of liquid particles in the wave.

Keywords**—**Flat-bottomed boat, Underwater wing, Input and output nozzles, Wave thrust, Conversion of wave into a jet stream, Oscillatory motion and onward motion, Squid-like pump, Hatch-like pump, The thrust due to lifting float, The thrust due to radiation reaction.

I. Introduction

MANY variants of more or less successful attempts of conversion of oscillatory motion or vibration of fluid or friable media (or devices, which was submerged into these media, i.e. vibrocarriers) into its onward motion are presented in literature [1-3]. Wave thrust (for the waves on surface of water) presents the special part of mentioned above area of investigations. One can obtain the average onward motion of a floating device in water waves due to the difference of water resistance for a mutually opposite directions of movement of device. But the averaged onward velocity (and also instant oscillatory velocity) of this motion can't exceed the velocity of liquid particles in wave (analogously for streams, created by powerful sound in liquid). Surfing is well known way to get fast onward motion, caused by a sliding of board along the running frontier of surface water wave due to the tangential component of gravity force. But this variant of onward motion is too defined by the concrete instant shape of surface wave and can't be used for aims of transport. Another approach of sliding uses the submerged wings (or fins), attached to a floating boat. Due to the special control of a wing inclination, we periodically obtain unidirectional horizontal component of lift force, caused by the vertical movement of liquid particles in wave [4-12]. The value of wave thrust is increasing with the value of wings surface. But large sizes of wings lead to technical difficulties. Intensity of surface wave is decreasing with depth of wings. Control can't be sufficiently fast, due to water masses, attached to the wing and without use of external energy sources. And the last example of approach of sliding – onward motion of a snake (or fish) in a hard slippery tortuous channel (created by same snake in liquid) [13], but with use of snake's energy of course. The abovementioned versions of approach of sliding do not create a jet spurts. These versions supposed the support like a slippery smooth oscillating surface of a "hard body" (i.e. the shape of surface does not depend on the above mentioned devices). Sliding floating devices, which were described in [4-12], can give the thrust only at pitching, but not at rolling. Below we will explore jet motion of a boat of special construction, due to which we can get thrust both at pitching and at rolling. At first we will describe the model construction with main results of testing, then – four possible physical mechanisms of boat jet motion and thrust.

II. Construction of the Model

General view of the tested model of a boat is presented in photograph in Fig. 1. This flat-bottomed model consists of three main details: the light slab 1 (hull), the cylindrical underwater wing 2 at the stern, the keel 3 at the bow (see also Fig. 2 with draft of the model [14, 15]). These three simple details provide the onward motion of a model, due to the lifting mechanism of creation of wave thrust (see section IV-E below) at least.

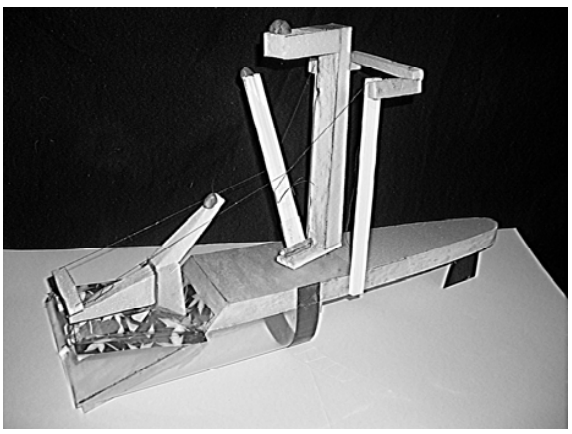

Fig. 1 Photo of the self-propelled boat model

The construction of model of boat includes: plane slab 1 (Fig. 2), keel 2 (Fig. 2), cylindrical elastic underwater wing 3 (Fig. 2, Fig. 3,d,e,f), rigid contour 4 of input nozzle (Fig. 2), flexible output nozzle, lavsan film 5 (Fig. 2, Fig. 3,a,b,c,f), the

cut 6 in the film 5 (Fig. 2, Fig. 3,a,b,c,f), rigid petal 7 (Fig. 2, Fig. 3,b), rigid floats 8 (Fig. 2, Fig. 3,c), rigid floats 9 (Fig. 2, Fig. 3,c), rigid floats 10 (Fig. 2, Fig. 3,c), lines 11 of bending (Fig. 1, Fig. 3,b,e,f), oscillator 12 of petal 7 (Fig. 2), supports 13 (Fig. 2), the rotating column 14 (Fig. 2), horizontal parts 15 and 16 of column 14 (Fig. 2), the rotating oscillator 17 (Fig. 2), concentrated masses 18 (Fig. 2), the non-extensible threads 19 (Fig. 2). There $L = 0.48$, $H = 0.1$, $h_1 = 0.19$, $h_2 = 0.05$ in Fig. 2. Total mass of model is equal to 0.11. Here and below the SI is used for the representation of all concrete values.

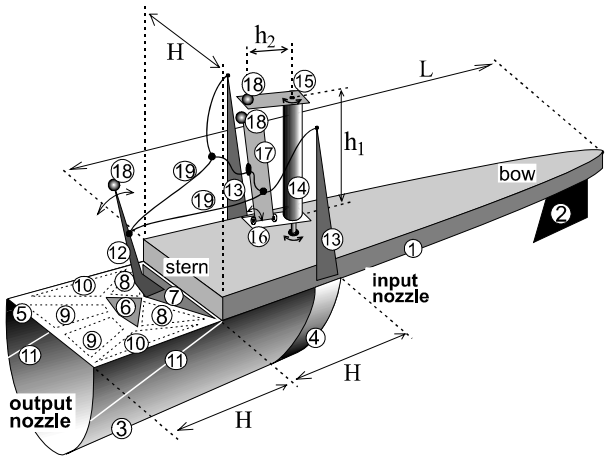

Fig. 2 General view to the construction of the model (draft)

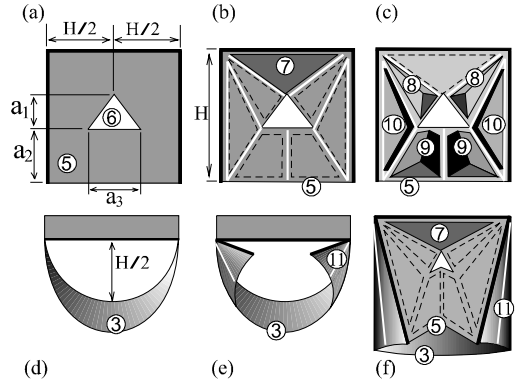

Fig. 3 The structure of the stern of boat: (a) thin weightless non tensile flexible lavsan film 5 with cut 6, where $a_1 = 0.02$, $a_2 = 0.045$, $a_3 = 0.025$, $H = 0.1$; (b) the top view of the film 5, the white lines for functional flexions for the film 5, the central hard petal 7, the dotted contours of the floats 8, 9, 10; (c) the look from below and the hard floats 8, 9, 10, attached to film 5; (d) the back view of the stern and underwater cylindrical wing 3; (e) the back view of the wing 3 at shrinking, the white lines 11 to help the flexions; (f) top view of wing 3 and of film 5 at shrinking

The underwater wing 3 (with rigid contour 4) is attached rigidly to the slab 1 (hull, foam plastic). The keel 2 is attached to the bow rigidly. The keel 2 provides (together with the wing 3) the stability of direction of onward movement of boat. The edge of the wing 3 (with contour 4) presents the input nozzle for sucking water. Another edge of wing 3 is presenting the output nozzle for injecting water spurts. Film 5 is attached (adhesively) to the borders of wing 3 and to the stern end of hull 1. The floats 8, 9, 10 (foam plastic) with the light rigid petal 7 are attached (adhesively) to the film 5. Oscillator 12 with tuned point mass 18 is attached rigidly to the petal 7. Lines 11 are placed on the wing 3 and film 5 for the more easy flexions at shrinking and expanding of output nozzle of boat. The rotating column 14 (foam plastic) with rigidly attached horizontal parts 15, 16 (with tuned point mass 18) and the rotating oscillator 17 (with tuned point mass 18), which fasten to the part 16 by hinges, are designed for the receipt of energy of rolling. The supports 13 are rigidly attached to the slab 1 (hull). The two threads 19 give the mechanical connection between oscillators 12 and 17 and provide the conversion of the energy of oscillations into the groups of pulses of shrinking of the output nozzle.

III. Results of Model Testing

Model (Fig. 1) of boat was tested in the experimental tank with stationary water wave field with vertical shifts of surface $\bar{u}_\perp(x, y, t) = A\cos(\omega t)\cos(kx)$ for a pitching and $\bar{\bar{u}}_\perp(x, y, t) = A\cos(\omega t)\cos(ky)$ for a rolling, where, $\omega = 2\pi / T$ –angle frequency, $k = 2\pi / \lambda$ –wave number, T –wave period λ –wavelength, A –wave magnitude. At the approach of deep water the magnitude of velocity of horizontal shifts of liquid particles in the wave field is equal to $U = \omega A$ and phase velocity of waves is equal to $c = \sqrt{g / k}$, where $g = 9.8$.

A. Review of Experimental Results

We measured in experiments: the instant horizontal move $\bar{U}(t)$ of the model along the axis "x" at pitching (Fig. 4,a), the instant horizontal move $\bar{\bar{U}}(t)$ of the model along the axis "y" at rolling (Fig. 4,b), the instant values of the forces $\bar{\mathbf{F}}(t)$ (Fig. 4,c) and $\bar{\bar{\mathbf{F}}}(t)$ (Fig. 4,d) of thrust of waves (along the boat axis) at pitching and rolling respectively, for the constant magnitude $A = 0.027$ of water waves and for several values of the wavelength λ (or for several wave periods T).

The value of onward velocity (average on period $T = 0.8$) of boat was $\left|< \bar{\mathbf{V}} >\right| = 0.83$ at pitching and $\left|< \bar{\bar{\mathbf{V}}} >\right| = 0.63$ at rolling. The peak values of boat velocity were $\left|\bar{\mathbf{V}}(t)\right|_{\max} = 4.17$ at pitching and $\left|\bar{\bar{\mathbf{V}}}(t)\right|_{\max} = 2.94$ at rolling, peak values of wave thrust were $\left|\bar{\mathbf{F}}(t)\right|_{\max} = 1.6$ at pitching (Fig. 4,c) and $\left|\bar{\bar{\mathbf{F}}}(t)\right|_{\max} = 1.1$ at rolling (Fig. 4,d). Phase velocity of water waves was $c = 1.24$, magnitude of velocity of horizontal shifts of liquid particles in the wave field was

$U = 0.21$ for $T = 0.8$. The force of the wave thrust (average on period $T = \lambda / c$) at pitching $\left|< \overline{\mathbf{F}} >\right|$ and at rolling $\left|< \overline{\overline{\mathbf{F}}} >\right|$, as the function of the wavelength λ, is presented in Fig. 5.

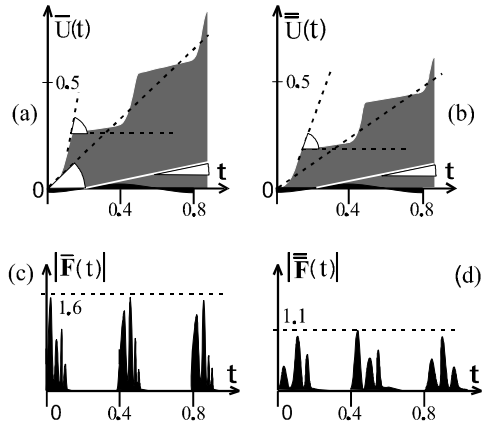

Fig. 4 The plots of boat horizontal coordinates $\overline{U}(t)$, $\overline{\overline{U}}(t)$ (freely floating boat) at pitching (a) and at rolling (b); the force $F(t)$ of the wave thrust for a horizontally fixed boat in the point $x = 0$ at pitching (a) and for a horizontally fixed boat in the point $y = 0$ at rolling (d) ($T = 0.8$, $\lambda = 0.99$, $A = 0.027$, $U = 0.21$)

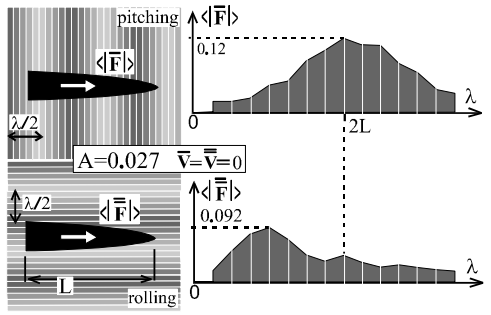

Fig. 5 The experimental plots of the wave thrust $< F >$ of model (at pitching and rolling) as function of the wavelength λ in regime of stationary sinusoidal waves, on the condition $\overline{U}(t) = \overline{\overline{U}}(t) = 0$

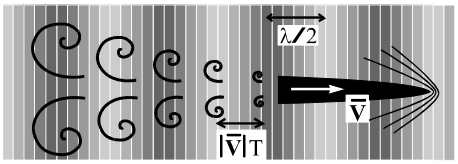

Fig. 6 The vortexes sequence behind stern of the model at pitching and water surface perturbations near the bow at jerks

B. Notes Concerning the Testing of the Model

On the basis of the lot of empirical facts, we can make the following five notes:

(1) The propulsive device above described (spaced on the stern of boat) can only push boat, but can't pull (if spaced at the bow, for instance).

(2) The magnitude $< \overline{\mathbf{F}} >$ of wave thrust of boat depends on magnitude and frequency of water waves. But at low velocities $\left|< \overline{\mathbf{V}} >\right| << c$ the magnitude of wave thrust of boat does not depend on the choice of relations $< \overline{\mathbf{V}} > \uparrow\uparrow \mathbf{k}$ (and $< \overline{\mathbf{F}} > \uparrow\uparrow \mathbf{k}$) or $< \overline{\mathbf{V}} > \uparrow\downarrow \mathbf{k}$ (and $< \overline{\mathbf{F}} > \uparrow\downarrow \mathbf{k}$) for running sinusoidal wave field (i.e. there is no difference in the thrust force between the cases, when waves run along the boat and when waves run against the boat) and for the stationary waves ($\mathbf{k}$-vector of a wave propagation, $k = |\mathbf{k}|$-wave number). The boat produces desired jets spurts, when the water surface (along the boat) is curved maximally and wave "tries" to break the plane slab 1 at pitching (i.e. when $L \sim \lambda / 2$). Besides this, the curvature of water surface near the boat must be changing also in time for the creation of wave thrust $< \overline{\mathbf{F}} > \neq 0$ at pitching. In other words we have $\left|< \overline{\mathbf{F}} >\right| = \max$ when $\left|(\partial / \partial t)(\partial^2 / \partial \xi^2)\overline{u}_\perp\right| = \max$, where $\xi = x - t\left|< \overline{\mathbf{V}} >\right|$. So in the regime of the waves, running in direction from the stern to the bow (at $< \overline{\mathbf{V}} > \uparrow\uparrow \mathbf{k}$), we would have obtained $< \overline{\mathbf{F}} >= 0$ (when $\left|< \overline{\mathbf{V}} >\right| = c$), for the pitching.

On the other hand the oscillatory rotation of the column 12 (Fig. 2) generates fast pulses of shrinking of output nozzle (and jet spurts) also at rolling, when water surface is not curved along the boat. In this case, we can get $\left|< \overline{\overline{\mathbf{F}}} >\right| = \max$, when $\left|(\partial / \partial t)(\partial / \partial y)\overline{\overline{u}}_\perp\right| = \max$, and $\left|< \overline{\overline{\mathbf{F}}} >\right| = 0$, when $\left|(\partial / \partial t)(\partial / \partial y)\overline{\overline{u}}_\perp\right| = 0$ on the line $x = const$, where the boat is placed.

(3) All details of propulsion device, sensitive to the wave, should be placed closely with water surface, as possible (as details 7–10 in Figs. 2, 3 for instance). These details, being sufficiently submerged in water, would take additional water mass (attached mass of water). This mass (or moment of inertia) does not permit the sufficiently quick move of these details in accordance with process on water surface, where the wave energy is concentrated. When testing boat at pitching, the rotating column 14 (Fig. 2) was fixed in neutral position.

(4) There was the difficult condition of chosen approach: we can not use any electronic details in the boat construction to exclude any speculation about outside energy supply to this boat in demonstrations of the effect of the wave thrust.

(5) The boat model has no details, which are immediately pushing the water similarly as oars, paddle wheel or screw propeller. So the proposed device can be characterized as a uniflow wave jet engine.

IV. Physical Mechanisms of Jet Motion and Thrust of the Boat Model

Concrete construction of a boat was groped empirically in a lot of experiments. However below we present several theoretical reasons and foundations for the construction chosen. We can note four physical mechanisms of the wave

thrust. Average (temporal) force $< F >$ of wave thrust we present roughly as a sum of four components, which denote these physical mechanisms:

$$< \mathbf{F} > \approx < \mathbf{F}_S > + < \mathbf{F}_H > + < \mathbf{F}_R > + < \mathbf{F}_L >, \qquad (1)$$

where $< \mathbf{F}_S >$ denotes the squid-like mechanism of thrust (section III-B), $< \mathbf{F}_H >$ denotes the hatch-like mechanism of thrust (section III-C), $< \mathbf{F}_R >$ denotes the radiation mechanism of thrust (section III-D), $< \mathbf{F}_L >$ denotes the lifting mechanism of thrust (section III-E). Among these components only two ($< \mathbf{F}_S >$ and $< \mathbf{F}_H >$) are acting both at pitching and rolling: the rest components ($< \mathbf{F}_R >$ and $< \mathbf{F}_L >$) work only at pitching. In addition to presentation of the results of testing in section III below we will describe the role of each detail of a boat in the process of creation of the wave thrust.

A. About Surface Sources of High Velocities of Jet Flows

We consider the approach of deep water, when magnitude of horizontal shifts $\mathbf{u}_{//}(x, y, t)$ and magnitude of vertical shifts $\mathbf{u}_{\perp}(x, y, t)$ of surface liquid particles are identical, i.e. $\left|\mathbf{u}_{//}(x, y, t)\right|_{\max} = \left|\mathbf{u}_{\perp}(x, y, t)\right|_{\max} = A$. Phase velocity of surface waves is equal to $c = gT / 2\pi$, where T –period of sinusoidal waves.

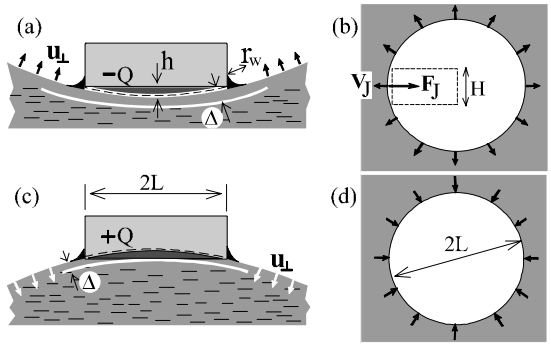

Fig. 7 The weightless hard disk spaced on the quasi-plane surface of water: side view of disk (a, c) with normal displacements $\mathbf{u}_{\perp}$ of water surface in wave; view from the top (b, d) with tangential (horizontal) velocities $\mathbf{V}_J$ of jet streams

Physically the thrust of boat, moving with velocity V, in accordance with the law of saving of mechanical impulse, can be caused by the jet streams (of velocity $V_J > V$), which are issued from the stern of boat (besides the variant of thrust, which is described in section III-E below). To get the desired relation $V > U$ we must ensure $V_J > V > U$ at least, where $V_J = \left|\mathbf{V}_J\right|$, $V = \left|\mathbf{V}\right|$, $\mathbf{V}$, $\mathbf{V}_J$ –vectors of velocity of boat model and velocity of liquid particles in the jet pulses respectively, $U = 2\pi A / T$ - magnitude of velocity of liquid particles in a wave on the water surface.

We consider the hard weightless disk on the water surface curved by waves with magnitude A of vertical shift. Also we assume for simplicity the stationary wave field with radial symmetry: $\mathbf{u}_{//}(x, y, t) = \mathbf{u}_{//}(r, t)$, $\mathbf{u}_{\perp}(x, y, t) = \mathbf{u}_{\perp}(r, t)$, where $r = \sqrt{x^2 + y^2}$. In this case under the disk we have the temporal sequence of water surfaces: convex (Fig. 7,c), concave (Fig. 7,a), convex, concave ... and so on with period T. Due to phenomena of adhesion between disk surface and water surface with wetting radius $r_w \approx \sqrt{\sigma / \rho g} << L$, disk gathers (Fig. 7,a,b) and pushes out (Fig. c, d) the liquid volume $\pm Q = \pi^5 g^{-2} L^4 T^{-4} A$ with height $h = 2\pi^4 g^{-2} L^2 T^{-4} A$ periodically ($\sigma \approx 7.3 \times 10^{-4}$ –coefficient of surface tension of water, $\rho = 10^3$ –mass density of water, L –radius of disk). Now we estimate roughly the velocity of streams on the intervals of gathering (Fig. 7,a,b) and pushing out (Fig. 7,c,d) under assumption that these streams are concentrated in the laminar boundary layer with thickness $\Delta \approx \sqrt{\nu T / 2\pi}$ ($\nu = 10^{-6}$ –coefficient of water viscosity). Now we cut the part of disk (dotted line in Fig. 7,b means the contour of a boat and prototype of the last) with width H and length L and we will try to estimate the corresponding jet velocity and reactive force of jet stream. The reactive force $\mathbf{F}_J$ of jet stream is connected with velocity $\mathbf{V}_J$ of jet stream by the formula $\mathbf{F}_J = -q\mathbf{V}_J$, where $q = (\rho H \Delta) V_J$ –water mass expense via the cross-section $H \times \Delta$. Averaging on half period $T / 2$, we obtain the following rough simple estimates of velocity of jet stream (Fig. 7,b, d)

$$V_J \approx 2^{3/2} \pi^{9/2} g^{-2} \nu^{-1/2} L^2 T^{-11/2} A^2 \qquad (2)$$

and the reactive force of jet streams

$$F_J \approx 2^{5/2} \pi^{17/2} g^{-4} \nu^{-1/2} \rho H L^5 T^{-21/2} A^3, \qquad (3)$$

caused by finite width $H << L$ of sector of disk (Fig. 7,b), where $F_J = \left|\mathbf{F}_J\right|$. We must note the significant relation between jet velocity V_J and velocity U of liquid particles in wave

$$V_J / U \approx 2^{1/2} \pi^{7/2} g^{-2} \nu^{-1/2} T^{-9/2} L^2 A \qquad (4)$$

and two qualitative nonlinear dependences $V_J \sim A^2$ and $F_J \sim A^3$. After substitution of $T = 0.8$, $L = 0.48$, $H = 0.1$ (parameters of waves and boat model) into (2-4) we obtain $V_J \approx 4.0 \times 10^3 A^2$, $F_J \approx 2.8 \times 10^5 A^3$, $V_J / U \approx 5 \times 10^2 A$.

If we will add to the problem, presented in Fig. 7, the special control (in accordance with wave) of oblique orientation of disk in a small angle area about $\pm h / L$, we

would get nonzero integrals (around the disk) of V_J and F_J, and onward motion of the disk consequently. Above consideration was based on continuous flows with large temporal scale $\sim T$. Pulsed spurts with temporal scale $\tau << T$ will have higher V_J and F_J.

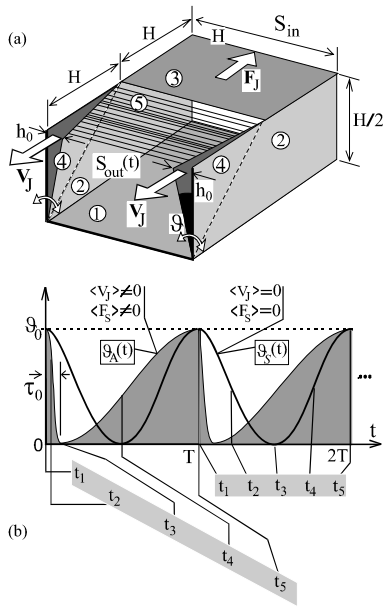

Fig. 8 Squid-like pump: (a) prototype of the underwater wing (presented in Fig. 2); (b) the symmetric $\vartheta_S(t)$ and asymmetric $\vartheta_A(t)$ trajectories of angle ϑ temporal changes of borders 1 of the squid-like pump

B. Squid-Like Pump Mechanism of Thrust of Boat.

Now we consider the forming of the component $< \mathbf{F}_S >$ of wave thrust in (1) and the construction of squid-like pump [16], presented in Fig. 8,a. Rigid details 1, 2, 3 are connected hardly. Rigid detail 4 is connected by hinges with rigid detail 2. Plane 3 is identical with the free surface of calm water (incident waves are absent). Rectangular combination of rigid details 1-4 (Fig.8,a) presents the prototype of the underwater wing 3 in Fig. 2. We assume roughly that the spurts are concentrated near the borders of details 4 in the layer of thickness of the order Δ (Fig. 7,a,b), when details 4 are squeezing out the water from output nozzle at shrinking. We assume roughly that the spurts are concentrated near the borders of details 4 in the layer of thickness of the order (Fig. 7,a,b), when details 4 are squeezing out the water from output nozzle at shrinking. The coupled mass (about $\sim H^3\rho/2$) of water under the detail 3 does not pass spurts, created by details 4, to the input nozzle (when output nozzle is shrinking). The action of construction in Fig. 8 represents the periodical sequence of fast shrinking (during the intervals $nT \le t < \tau_0 + nT$, $n = 0,1,2,...$, T –period) and slow expanding (during the intervals $\tau_0 + nT \le t < \tau_0 + (n+1)T$, $\tau_0 << T$) of output nozzle with variable area of cross-section $S_{out} = S_{out}(t)$. Cross-section area $S_{in} = const$ of input nozzle remaines constant. The position of detail 4 is described by angle $\vartheta(t)$. Fig. 8,b represents the examples of symmetric and asymmetric temporal trajectories $\vartheta_S(t)$ (with $\tau_0 = T$) and $\vartheta_A(t)$ (with $\tau_0 << T$) of change of ϑ. Two distributions of the moments $t_1 < t_2 < t_3 < t_4 < t_5$ (points, when functions $\vartheta_S(t)$, $\vartheta_A(t)$, achieve the same values ϑ) are shown in Fig. 8,b. The velocity V_J of jet spurt and the reactive force F_J change its signs together with the sign change of $(d/dt)\vartheta$. So the impulse of reactive force (average on period $< \mathbf{F}_J >$, and also the average spurt $< \mathbf{V}_J >$ via S_{out}) becomes zero for the symmetric trajectory $\vartheta_S(t)$. In other words for $\vartheta_S(t)$ we obtain the relation $\left[|\mathbf{I}_+|/|\mathbf{I}_-|\right]_{\vartheta=\vartheta_S(t)} = 1$ of impulses $\mathbf{I}_+ = \int_0^{\tau_0} \mathbf{F}_J dt$, $\mathbf{I}_- = \int_{\tau_0}^{T_0} \mathbf{F}_J dt$ of reactive force. On the other hand for the asymmetric trajectory $\vartheta_A(t)$ we obtain $\left[|\mathbf{I}_+|/|\mathbf{I}_-|\right]_{\vartheta=\vartheta_A(t)} > 1$. Using the formula (3), we can estimate this relation roughly (with analogy $A \sim \vartheta_0 H/2$, ϑ_0 is shown in Fig. 8,b) $\left[|\mathbf{I}_+|/|\mathbf{I}_-|\right]_{\vartheta=\vartheta_A(t)} \sim \left[(T-\tau_0)/\tau_0\right]^{21/2} >> 1$. In accordance with the construction of the boat, the period T can be wave period or period of pitching or rolling. We did not take into account the producing of water waves by the oscillatory motions of details 4, because the area of wing is much shorter, than the wavelength, i. e. $H << \lambda = (g/2\pi)T^2$ and represents the area of hydrostatic description of vertical shifts of water surface.

C. Hatch-Like Pump Mechanism of Thrust of Boat

Here we consider the analog of device, described above, with some difference: rigid plane rectangular walls 1, 2, 3, rigidly connected, plus the hatch 4 (connected by hinges with detail 3, Fig. 9,a). This construction is also the prototype of underwater wing (presented in Fig. 2) with cross-section areas of input nozzle $S_{in} = const$ and output nozzle $S_{out} = S_{out}(t)$. The plane 3 is identical with the free surface 5 of water, as above. We assume that the hatch 4 is weightless and can change the orientation angle ϑ: at horizontal moistened hatch we get $\vartheta = 0$. Below we assume that hatch is connected to some source of vertical force $\mathbf{F}_T$ via some thread, weightless, flexible and non-extensible. In initial position at moment $t = t_1$ (Fig. 9,b) we have $\mathbf{F}_T = 0$ and free tread. Then, at moment $t_1 < t < t_2$, we switch on the force $|\mathbf{F}_T| > 0$. Thread

becomes tensed, the hatch (with meniscus) is getting up ($\vartheta > 0$) together with finite mass (about $\sim H^3\rho/2$), of water connected by adhesion with the hatch. Simultaneously this amount of water, moved by hatch, has the horizontal velocity component, due to the linear distribution of vertical velocities of liquid particles on the moistened surface of rotating hatch and due to the centrifugal volume forces in liquid. The lifting of hatch (and of water, connected with hatch) will be continued till the moment $t = t_4 > t_3$, when the gravity force will exceed the vertical component of the adhesive force. Hatch is tearing from the water surface, the thread becomes free and force $\mathbf{F}_T$ becomes zero.

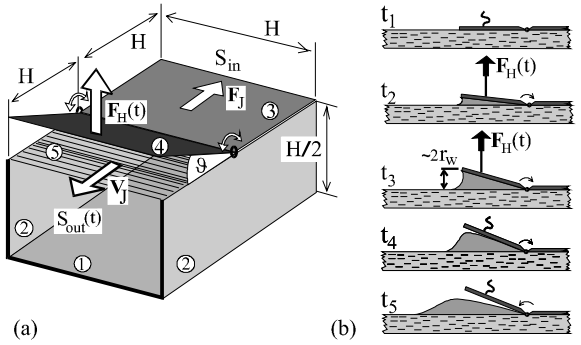

Fig. 9 Hatch-like pump: (a) prototype of the underwater wing (presented in Fig. 2); (b) the functional phases of the hatch-like pump mechanism at the moments $0 < t_1 < t_2 < t_3 < t_4 < t_5 < T$

The main part of water, which was previously pulled up by hatch, is moving to the left (Fig. 9, b, $t \geq t_4$). This experimental fact causes the nonzero component $< \mathbf{F}_H >$ of wave thrust (1). Then hatch is falling freely on the water surface (Fig.9,b). When the previously formed "hill" of water has relaxed, the source of the vertical force $\mathbf{F}_T(t)$ is switched on again, and the operations, described above, are repeated periodically with period T.

D. Radiation Pressure Mechanism of Thrust of Boat

This section is devoted to the known phenomenon of radiation pressure [17, 18], in the view of the problem of a wave thrust, i.e. the component $< \mathbf{F}_R >$ in (1). The experimental setup for exploration of radiation pressure is presented in Fig. 10,a. Radiator presents two floats A and B, rigidly connected with each other (catamaran, maden of foam plastic), equipped with four vibrators in the form of rotating masses. Pair of masses on each float is rotating in antiphase for the mutual compensation of horizontal forces. Both axis of rotation with pairs of vibrators are excited by one electric drive. So all vibrators are rotating with the same angle frequency ω_0, but with phase difference $\pi/2$ between floats A and B. Therefore the phase difference between forces of vertical vibration of A and B is $\pi/2$ also. We neglect the mass of motor and floats and we can conclude that difference between phases φ_A and φ_B of vertical oscillatory velocities (and also vertical shifts) of the floats A and B is approximately the same, i.e. $\pi/2$.

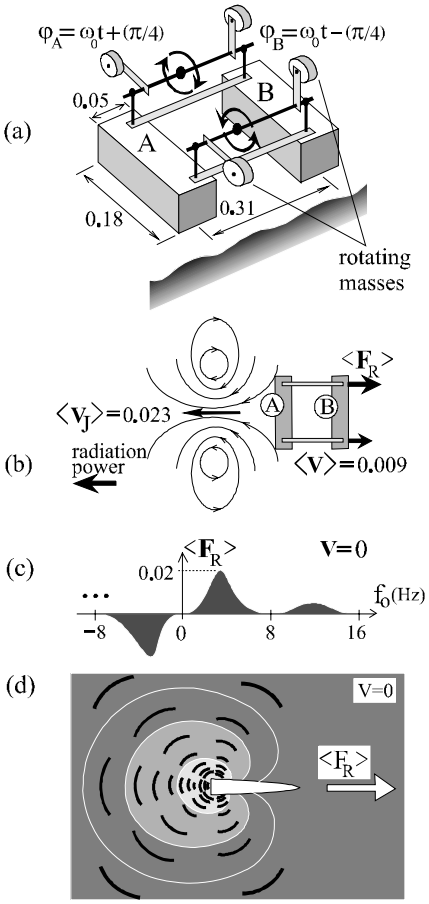

Fig. 10 Mechanism of radiation pressure: (a) construction of floating radiator (propeller); (b) top view of a jet stream, caused by vibration of radiator; (c) frequency dependence of the wave thrust (average on period $2\pi/\omega_0$) of catamaran; (d) anisotropy of radiation wave field of a boat model, caused by pitching

The top view of the streams on water surface near the radiator is presented in Fig. 10,b with characteristic value of the jet stream velocity $< \mathbf{V}_J >$ (average on period $2\pi/\omega_0$ (or $1/f_0$) vibration of catamaran) and velocity $< \mathbf{V} >$ (average on the same period) of onward self propelled motion of radiator on the frequency $f_0 = 3.8$ Hz and when magnitude of vertical oscillatory shifts of a floats is equal $A_0 = 0.02$. This frequency corresponds the distance between floats A and B, equal $1/4$ of the wavelength λ on the surface of deep water. This is a classic case of unidirectional radiation. Direction of main power stream of radiation is the same with direction of the jet stream.

The frequency dependence of the force $< \mathbf{F}_R >$ (average on

period $1/f_0$) of radiation thrust is presented in Fig. 10,c and was measured, when the condition $\mathbf{V}=0$ was supported. Negative frequencies in Fig. 10,c mean the opposite direction of rotation of electric drive in the radiator, and this lead to the opposite direction of wave thrust force and velocity of onward motion of radiator (i.e. change $f_0 \to -f_0$ means the changes $<\mathbf{F}_R> \to -<\mathbf{F}_R>$, $<\mathbf{V}_J> \to -<\mathbf{V}_J>$, $<\mathbf{V}> \to -<\mathbf{V}>$).

The interaction between weakly curved (by waves) surface of water with bottom plane of boat model can be characterized like a sequence of sliding blows. So the oscillations (pitching) of boat can be presented by discrete frequencies $\omega_n = n\omega_w$ ($n=1,2,3...$) in addition to the frequency ω_w of initial wave field. Due to this fact the force of radiation reaction $<F_R>$ arises, which we estimate roughly as $<F_R> \sim \sum_{n=1}^{\infty} c^{-1}(\omega_n)\Pi(\omega_n)$, where $c(\omega_n)=g/\omega_n$ is phase velocity of the surface water waves of the frequency ω_n, $\Pi(\omega_n)=\overline{W}_n-\overline{\overline{W}}_n$, $\overline{W}_n=\int_0^{\pi/2}\Psi(\omega_n,\vartheta)\cos\vartheta d\vartheta$ –stream of power from the stern ($0\le|\vartheta|<\pi/2$), $\overline{\overline{W}}_n=\int_{\pi/2}^{\pi}\Psi(\omega_n,\vartheta)\cos\vartheta d\vartheta$ –stream of power from the bow ($\pi/2\le|\vartheta|<\pi$), $\Psi(\omega_n,\vartheta)$ –azimuthal distribution of the density of stream of radiation power in far zone ($0\le\vartheta<2\pi$). Radiation directivity pattern $\Psi(\omega_n,\vartheta)$ is more narrow function of ϑ at more high frequencies ω_n. We estimate roughly the total power $\overline{W}_n+\overline{\overline{W}}_n=W(\omega_n)$, radiated by a boat, on frequency ω_n, as the expression $W(\omega_n)\sim(A\omega_n/2\pi)^2\,\mathrm{Re}\,Z(\omega_n)$, where $\mathrm{Re}\,Z(\omega_n)\sim|\omega_n|^7$ is the radiation resistance [19] for the small ($L<\lambda$) boat as oscillator on deep water. The values c^{-1},Ψ are growing together with frequency ω_n. Therefore the pulsing regime of boat oscillations gives greater force $<F_R>$ of radiation reaction, as a sum of positive contributions on each frequency ω_n. Of course we assume $c(\omega_n)>>V$, and consider not too high frequencies, for which we can neglect the viscosity effect.

The slab 1 and the wing 2 (Fig. 2) are the main details of a model in the radiation mechanism of wave thrust. The bow of model is of very small weight and follows exactly the vertical oscillatory shifts of liquid particle in the wave field. The stern of a boat has a coupled mass of water (with effect only on vertical oscillations), due to which the vertical oscillation of the stern is delayed in comparison with the oscillation of the bow with time delay about $T_1/4$ (where T_1 is a period of pitching). At the length $L\approx\lambda_1/4$ (where λ_1 is a wavelength corresponding the period T_1 of pitching) of slab 1, the boat gives about 80% of total radiation power to the back half-space (from stern of a boat). The picture of radiation wave field, created by the pitching of boat, is presented in Fig. 10,d.

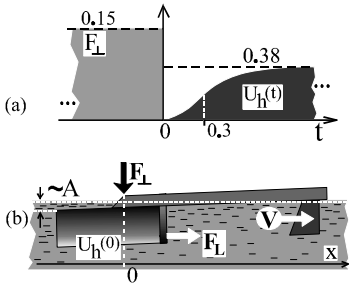

Fig. 11 Lifting mechanism of the thrust: plots of vertical force $\mathbf{F}_\perp$ and horizontal displacement $U_h(t)$ (a) at the oblique initial position of the model (b), i.e. at $t=0$ and $U_h(0)=0$

E. Lifting Mechanism of the Thrust.

To describe the forming of the component $<\mathbf{F}_L>$ in (1) below we consider the boundary problem at following initial conditions: water surface is plane (without waves), model is immovable, constant vertical force $\mathbf{F}_\perp$ is applied to the stern of model (Fig. 11,a). This force causes the oblique submersion of boat (Fig. 11,b). At moment $t=0$ the force becomes zero and boat begins its lifting. But due to the wing 3 (Fig. 2) this lifting is accompanied by horizontal displacement $U_h(t)$. Fig. 11,a presents the experimental plots of the force $\mathbf{F}_\perp(t)$ and displacement $U_h(t)$ for the concrete case. Now let's imaging the following situation: wave field pulls the boat's wing downward (with submersion of the order of water wave magnitude $\sim A$) periodically, and boat "tries" to lift simultaneously with forward movement $U_h(t)$. One can see, that for this movement (and for this thrust) the boat needs the water waves, propagating along the axis of boat. But the direction of movement (and the direction of thrust) does not depend on the direction of wave propagation (i.e. following waves or contrary waves). Lifting does not produce jet pulses and presents some analog of sliding mechanisms described in section I.

The average thrust force, which was created by lifting mechanism, we can estimate roughly as $<F_L>\sim(T_0/2T)(F_L)_{\max}$, where $F_L=|\mathbf{F}_L|$, $(F_L)_{\max}\approx(A/L)F_\perp$ is maximum value of horizontal component of the force $\mathbf{F}_L(t)$ of liquid action on the model at $t=0$, T is wave period, T_0, is the moment of the twist of

plot of $U_h(t)$ in Fig. 11,a, where $T_0 = 0.3$.

V. Conclusion

The plane bottomed boat construction does not limit very much the possible applications of this work. For instance this wave propelled boat can tow another boat of ordinary shape. And, in addition, this wave propelled boat can be controlled (steered by keel 2 in Fig. 2) without any crew, but only by the GPS navigator.

References

[1] I. .I. Blekhman, *Vibrational Mechanics*, Moscow: Fizmatlit Publishing Company, 1994.
[2] V. P. Boldin, A.I. Vesnitsky, E.E. Lissenkova, "An elementary wave propeller," Dokl. Akad. Nauk SSSR. vol. 318, no. 4, pp. 849-852, 1992.
[3] A. I. Vesnitsky, N.D. Romanov, G.A. Utkin, "About an efficiency wave propeller," Dokl. Akad. Nauk SSSR. vol. 306, no. 4, pp. 810-811, 1989.
[4] M. A. Lavrent'ev, B.V. Shabat, *Hydrodynamics Problems and their Mathematical Models*, Moscow: Science, 1977.
[5] V. V. Arabadzhi, "Wave-jet converters," *Journal of Low Frequency Noise and Vibration and Active Control*, vol. 21, no. 2, pp. 101-116, Apr. 2002.
[6] V. V. Arabadzhi, "On the conversion of boat pitching into a wave propulsion," Proc. 1-st WSEAS Int. Conf. MN'08, pp. 158-164, 2008.
[7] L. F. Kozlov, *The Theoretical Bio-Hydrodynamics*, Kiev, Head publishing holding "Visshaya shkola", 1983 (edited by N.T. Romanenko).
[8] V. G. Chikarenko, A. G. Gavryushin, "Efficiency of winged wave propeller devices," *Morskoi Flot*, no. 5–6, p. 22, 1994.
[9] G. E. Pavlenko, "Wave energy as a means of ship propulsion," *Sudostroenie*, no. 6, p. 394, 1936.
[10] I. K. Borodai, Yu. A. Netsvetaev, *Wave Motion of Ships*, Leningrad: Sudostroenie, 1969.
[11] Shigeru Naito, "Effect of bow wings on ship propulsion and motions", Appl. Mech. Rev., vol. 58, no. 4, 253-269, July 2005.
[12] http://www.utro.ru/news/2008/03/17/724180.shtml
[13] http://www.ecofuss.com/wave-propeller-boat-isnt-fast-but-loves-the-environment/
[14] http://nauka.relis.ru/17/9806/17806106.htm
[15] http://ru-patent.info/20/30-34/2034739html
[16] G. A. Konstantinov, Yu. L. Yakimov, "Calculation of the thrust of a wave-powered marine propelling device," Fluid Dynamics, vol. 30, no. 3, pp. May 453-456, 1995.
[17] James Lighthill, *Waves in Fluids*, Cambridge: University Press, Cambridge-London-New-York-Melbourne, 1978.
[18] M. E. McIntyre., "Myth of wave impulse", *Journal of Fluid Mechanics*, vol. 106, May 1981.
[19] L. N. Sretenski, *Theory of Liquid Wave Motions*, Moscow: Science, Phis.-Math. Publishing company, 1977.

V. Arabadzhi: Ph.D. in radiophysics 1994, senior researcher in the Institute of Applied Physics (Russian Academy of Sciences), 603950 Nizhny Novgorod, Ulianov st. 46, Russian Federation. Area of interests: wave thrust, reducing of acoustical and radio visibility of physical bodies. Fax: 7-(831)-436-59-76, E-mail: v.arab@hydro.appl.sci-nnov.ru .

His previous publications:

V. V. Arabadzhi, "On the active cancellation of ship waves," *Experiments in Fluids*, vol. 20, pp.225-226, 1996.
V. V. Arabadzhi, "Suppression of the sound field of a vibrating body by monopoles attached to its surface," *Acoustical Physics*, vol. 52, no. 5, pp. 592-600, 2006.
V. V. Arabadzhi, "Nonreflecting switching microstructure," *Journal of Communications Technology and Electronics*, vol. 50, no. 5, pp. 613-625, 2005.
V. V. Arabadzhi, "Algorithm for active suppression of radiation and acoustical scattering fields by some physical bodies in liquids," *Algorithms*, 2, pp. 361-397, 2009.